Pharmaceutical Research, Vol. 26, No. 1, January 2009 (© 2008)
DOI: 10.1007/s11095-008-9744-7

Research Paper

Loading PEG-Catalase into Filamentous and Spherical Polymer Nanocarriers

Eric A. Simone,[1,2,7] Thomas D. Dziubla,[3] Evguenia Arguiri,[4] Vanessa Vardon,[5] Vladimir V. Shuvaev,[2] Melpo Christofidou-Solomidou,[4] and Vladimir R. Muzykantov[2,6]

Received September 5, 2008; accepted October 2, 2008; published online October 28, 2008

Purpose. Based on a unique phase alignment that occurs during formulation, we postulated that PEGylation of the cargo enzyme would enhance its encapsulation within diblock copolymer nanocarriers and thus resistance to proteases.

Methods. A freeze–thaw modified double emulsion technique was utilized to encapsulate either the catalytically active enzyme catalase (MW ~250 kDa) or PEG-catalase in PEG–PLA polymer nanocarriers (PNC). Spectrophotometer measurement of substrate depletion was utilized to monitor enzyme activity. Isotope labeling of the enzyme was used in conjunction with activity measurements to determine PNC loading efficiency and PNC-enzyme resistance to proteases. This labeling also enabled blood clearance measurements of PNC-loaded and non-loaded enzymes in mice.

Results. Non-loaded PEG-catalase exhibited longer circulation times than catalase, but was equally susceptible to proteolysis. Modulation of the ratio of relatively hydrophilic to hydrophobic domains in the diblock PEG–PLA copolymer provided either filamentous or spherical PNC loaded with PEG-catalase. For both PNC geometries, encapsulation and resistance to proteases of the resultant PNC-loaded enzyme were more effective for PEG-catalase than catalase. Isotope tracing showed similar blood levels of PNC-loaded and free PEG-catalase in mice.

Conclusions. PEGylation enhances active catalase loading within PNC and resistance to protease degradation, relative to unloaded PEG-catalase.

KEY WORDS: antioxidant enzymes; filamentous carrier; encapsulation; PEG-catalase; polymer nanocarrier.

INTRODUCTION

Premature elimination from circulation, as well as inactivation by inhibitors and proteases, limit the effectiveness and utility of therapeutic enzymes. Coating with relatively hydrophilic poly (ethylene glycol) (PEG) prolongs circulation and reduces recognition of therapeutics and their carriers by defense systems (stealth technologies) (1–3). On the other hand, affinity targeting improves site-specific localization and drug efficacy. For example, through conjugation of an affinity antibody, targeting catalase (an antioxidant enzyme that dissociates the reactive oxygen species H_2O_2 into water and oxygen) to endothelial cells lining the blood vessel lumen alleviates vascular oxidative stress in animal models (4–7). However, targeted catalase-antibody conjugates traffic to lysosomes and are degraded by proteases within a few hours, terminating therapeutic effectiveness (8).

Therapeutic enzymes can be encapsulated within stealth polymer nanocarriers (PNC) in order to limit access to and degradation by lysosomal proteases (9,10). Inactivation of labile enzymes is a main challenge of PNC encapsulation (11,12). However, a double emulsion technique that involves a freeze–thaw cycle permits encapsulation of diverse, catalytically active enzymes including catalase (a large, MW ~250 kDa, highly labile tetrameric enzyme) into PEG-poly(lactic acid or lactic-co-glycolic acid) (PEG-PL(G)A) PNC (11,13). These PNC have diameters on the order of 300 nm that permit vascular administration. The catalase substrate, H_2O_2, diffuses through cell membranes and the PNC polymer materials with similar kinetics (14). Therefore, PNC act as a protective cage for the encapsulated enzyme, capable of sustained therapy without the need for drug release (11,13). *Ex vivo* perfused lung studies showed that targeting PNC-encapsulated catalase (antibodies conjugated directly to the PNC) to the endothelium provides sustained augmentation of antioxidant defense and

[1] Department of Bioengineering, University of Pennsylvania, Philadelphia, Pennsylvania 19104, USA.
[2] Institute for Environmental Medicine, University of Pennsylvania School of Medicine, 3620 Hamilton Walk, 1 John Morgan Building, Philadelphia, Pennsylvania 19104, USA.
[3] Department of Chemical and Materials Engineering, University of Kentucky, Lexington, Kentucky 40506, USA.
[4] Pulmonary Critical Care Division, Department of Medicine, University of Pennsylvania School of Medicine, Philadelphia, Pennsylvania 19104, USA.
[5] Department of Chemical Engineering, Drexel University, Philadelphia, Pennsylvania 19104, USA.
[6] Department of Pharmacology, University of Pennsylvania School of Medicine, Philadelphia, Pennsylvania 19104, USA.
[7] To whom correspondence should be addressed. (e-mail: esimone@seas.upenn.edu)

ABBREVIATIONS: DCM, dichloromethane; MW, molecular weight; PEG-cat, Peg-Catalase; PEG, poly(ethylene glycol); PLA, poly(lactic acid); PLGA, poly(lactic-co-glycolic acid); PNC, polymer nanocarrier; PVA, poly(vinyl alcohol); THF, tetrahydrofuran.

protection against vascular oxidative stress (13). Therefore, further investigation and optimization of this promising approach represent an important biomedical goal.

Of particular interest from this standpoint, Fig. 1 illustrates a unique phase alignment of the amphiphilic diblock copolymer PEG-PLA that occurs during the modified double emulsion at the oil/water interface (15). This phase separation is enhanced by the initial, primarily organic phase emulsion and the sharp temperature transition utilized in this formulation step (−80°C freeze–thaw). The relatively hydrophilic PEG block of the copolymer will preferentially distribute into the proportionately small fraction aqueous phase (primary emulsion is 90% oil phase) that contains protein due to PEG's ability to form hydrates with water, especially upon negative temperature transitions (16,17). It has also been shown that in addition to the formation of inverse micelles, PEG can enhance solubility in an oil phase, and this may further assist PNC loading of a protein in a w/o/w emulsion (18). Most likely, this effect will be proportional to a protein's hydrophilicity, which in turn, can be enhanced by its PEGylation. These considerations suggest that PEG-catalase may preferentially partition into PEG cores of the initial emulsion stabilized by the negative temperature transition (Fig. 1B). This would be an important advantage over the current double emulsion approach in which catalase encapsulation into PNC is associated with surface deposition of a significant fraction of the enzyme that is not protected from proteases (11,15).

The goal of this study was to test whether catalase replacement by PEG-catalase enhances the encapsulation efficiency and minimizes the surface accessible enzyme fraction in PEG–PLA PNC. Furthermore, we have reported recently that an increase of the hydrophobic PLA molecular weight fraction in the diblock PEG–PLA copolymer over 80% leads to formation of filamentous catalase-loaded PNC, while lower PLA content yields spherical carriers (15). Therefore, in this study we also examined PEG-catalase loading into morphologically different PNC. We characterized PNC/PEG-catalase drug delivery systems in terms of protein loading, morphology, activity and susceptibility of loaded enzyme to protease degradation, and circulation *in vivo* in a mouse model.

MATERIALS AND METHODS

Reagents

All chemicals and reagents, including PEG-catalase, were purchased from Sigma-Aldrich (St. Louis, MO, USA) and used as received unless otherwise stated. Methoxy-PEG (mPEG) MW 5,000 was purchased from Polysciences (Warrington, PA, USA). Catalase from bovine liver and horseradish peroxidase were purchased from Calbiochem (EMD Biosciences, San Diego, CA, USA). Uranyl acetate was acquired from Electron Microscopy Sciences (Fort Washington, PA).

Synthesis of Diblock Copolymers

DL–lactide was precipitated twice into anhydrous diethyl ether, before mixing with mPEG in stoichiometric ratios to achieve desired molecular weights. Reactants were purged with dry nitrogen and sealed in a round bottom flask before heated to 140°C while stirring for 2 h to remove trace water from samples. The temperature was reduced to 130°C and stannous octoate (1 wt.%) was added to catalyze the ring opening polymerization (ROP) of lactide with mPEG serving as the initiator. The polymerization was allowed to continue for 6 h. The diblock copolymer was then dissolved in DCM and twice precipitated in cold diethyl ether. Residual solvent was then removed by first drying *via* rotary evaporation (Safety Vap 205, Buchi, Switzerland), followed by lyophilization (VirTis BenchTop SLC, SP Industries, Gardiner, NY, USA).

Number average molecular weights $(\overline{M_n})$ of bulk copolymers were determined using proton nuclear magnetic resonance (^{1}H-NMR). The weight average molecular weights $(\overline{M_w})$ and polydispersity indices (PDI) were also determined by gel permeation chromatography (HPLC–GPC), with a Binary HPLC pump (1525, Waters, Milford, MA, USA), a Refractive Index Detector (2414, Waters) and three serial 7.8×300 mm Styragel columns (Waters) using tetrahydrofuran (THF) as the mobile phase. Chromatograms were analyzed using Breeze version 3.3 software with polystyrene standards used for calibration.

Diffusivity of Hydrogen Peroxide Through PEG–PLA

The diffusivity of H_2O_2 through PEG–PLA was determined with a two diffusion chamber apparatus, as described before (19). Briefly, for each experiment, a new thin polymer film was cast and the thickness measured, before placement between two chambers, the donor containing the substrate, 5 mM H_2O_2 in pH 7.4 50 mM phosphate buffered saline (PBS), and the receptor containing simply 50 mM PBS. The two-cell apparatus was maintained at physiologic temperature. The concentration of H_2O_2 in the receptor compartment was determined as a function of time by measuring UV absorbance at 242 nm (Cary 50 UV-Vis, Varian, Palo Alto, CA, USA).

Nanoparticle Formation

A freeze–thaw double emulsion solvent evaporation technique was used as previously outlined (11). Briefly, mPEG–PLA diblock copolymer is dissolved in DCM at 25 mg/ml. A 1 mg/ml catalase, or PEG-catalase (PEG $\overline{M_n} = 5,000$, ~40 PEG molecules per protein molecule according to supplier) solution and a PVA surfactant solution (2 wt.%, 87–89% hydrolyzed, $\overline{M_w} = 13,000 - 23,000$) in 20 mM PBS are prepared. The primary emulsion consists of the organic phase (1 ml polymer–DCM mixture) and the aqueous phase (100 µl catalase solution) homogenized at 15,000 rpm for 1 min in a dry ice–acetone bath with a 7 mm-blade homogenizer (Kinemetica Polytron 3100 with a PDTA3007/2 generator, Brinkmann Instruments, Westbury, NY, USA). The primary emulsion is then added to 5 ml of the PVA surfactant solution and homogenized at 15,000 rpm for 1 min. The resultant mixture is added to 10 ml of PVA solution and stirred overnight to allow removal of the residual solvent. The microparticle fraction is removed by a primary centrifugation at 1,000×*g* for 10 min. The nanoparticle fraction is collected by subsequent centrifugation at 20,000×*g* for 30 min. The supernatant is then removed and the PNC pellet is re-suspended in PBS and purified again by further centrifugation.

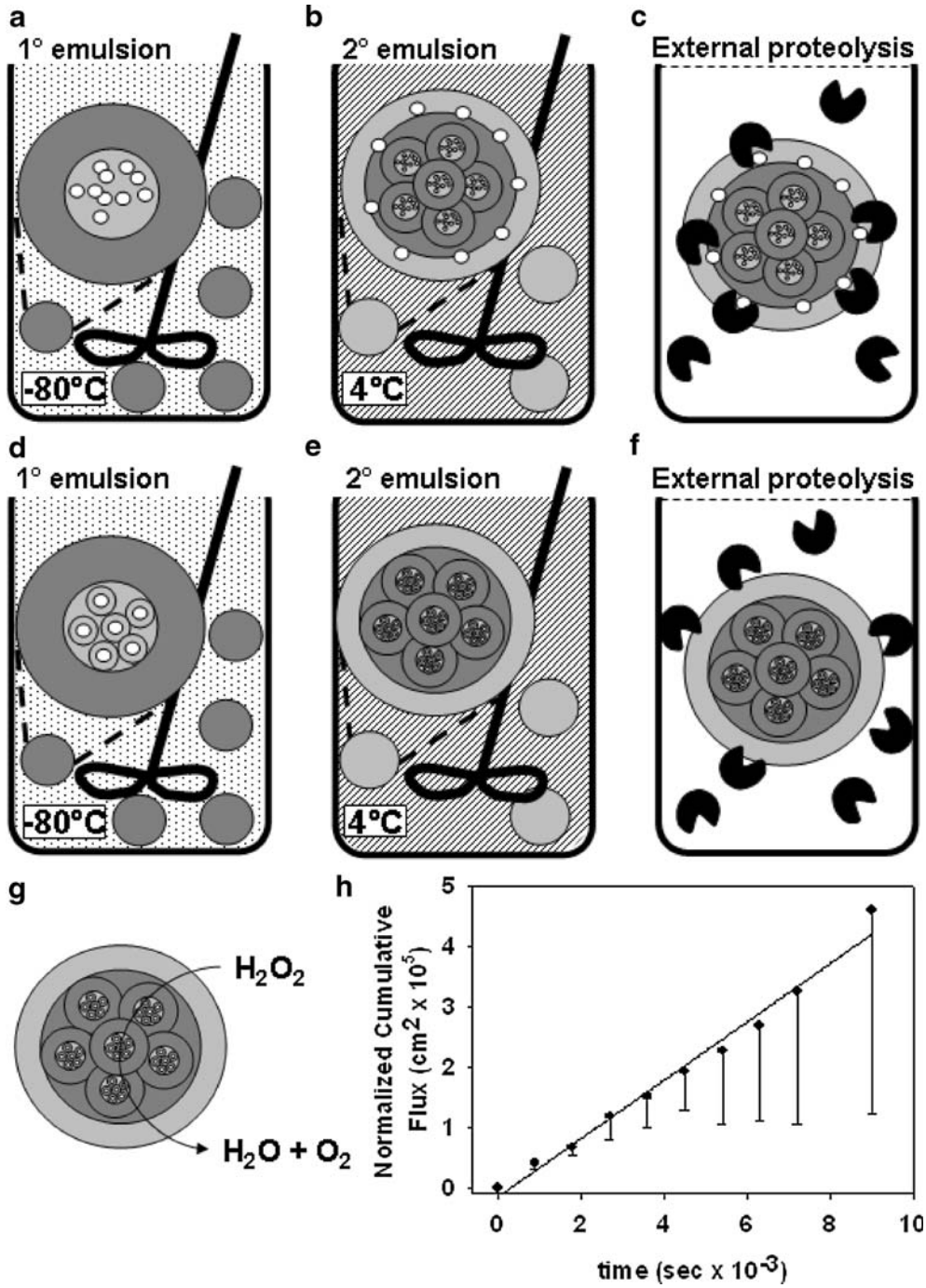

Fig. 1. Formulation and mechanism of therapeutic action. Schematic of freeze–thaw double emulsion PNC formulation (**A**–**C**) and how utilization of a PEGylated cargo changes this (**D**–**F**), namely enhancement of loading and reduction of surface accessible protein. *Light gray* indicates PEG and *dark gray* represents PLA. *White circles* are protein, and *white circles* with concentric *outer light gray ring* are PEGylated catalase. *Black dotted background* is the organic phase of the primary emulsion, and *black slashed background* is the aqueous surfactant secondary emulsion phase. In theory, during this freeze-cycle, the primary emulsion, 90% organic phase/10% aqueous phase, consists of inverse micelles of the amphiphilic diblock PEG-PLA copolymer with a PEG-core containing the hydrophilic enzyme. Thus we hypothesized that PEGylated proteins would preferentially distribute within these PEG cores, stabilized by the −80°C cycle. Furthermore, it is known that negative temperature transitions favor the formation of PEG hydrates and thus PEGylated catalase loading should benefit from the phase alignment of this synthesis scheme. For the therapeutic effect without cargo release, the key parameter is that the enzyme substrate (H_2O_2) diffuses freely through the PNC matrix (**G**). Diffusivity of substrate through polymer material is determined *via* a two chamber diffusion experiment, results of which are depicted (**H**). The diffusivity, or permeability coefficient, D, is the slope of the flux curve.

Enzyme Loading Determination

Protein loading was determined *via* radioisotope labeling and enzymatic activity. Loading *via* radiolabeling was determined as described before, by formulating PNC with ^{125}I-labeled catalase (11) or PEG-catalase. Catalase or PEG-catalase was radiolabeled with Na^{125}I (Perkin Elmer, Boston, MA, USA) *via* the Iodogen method (Pierce Biotech., Rockford, IL). Unbound ^{125}I was removed from the enzyme using Biospin 6 columns in accordance with the manufacturer's instructions (Bio-Rad labs, Hercules, CA, USA). Total ^{125}I-catalase in solution was measured before centrifugation, and then radioactivity of the ^{125}I-catalase/PNC-composed pellet after centrifugation was measured. A Wizard 1470 gamma counter (Wallac, Oy, Turku, Finland) was used for radiotracing.

To determine loading *via* enzymatic activity, a catalase activity assay (20,21) was used, both for the total sample before and after centrifugation. Briefly, 990 μl of 5 mM H_2O_2 in PBS and 10 μl of enzyme-loaded PNC was added to a quartz cuvette. The kinetics of H_2O_2 degradation was then measured with a spectrophotometer at 242 nm (absorbance at this wavelength corresponds to the H_2O_2 concentration and thus catalase activity, U/mg=23.0(ΔA_{242}/min) per milligram of catalase).

Catalase Protection Against Proteolysis

Protection against proteolysis was tested as described previously (11). Briefly, PNC preps loaded with ^{125}I-catalase were incubated with a 0.2 wt.% pronase solution at 37°C in a shaker bath set at 60 rpm for 1 h. Samples were removed and centrifuged at 16,000×*g* for 20 min. Supernatant containing degraded protein and pellet containing intact protein encapsulated within PNC were collected and counted. This measure correlates linearly with preservation of enzymatic activity (11,13).

PNC Size Determination

Size was determined *via* dynamic light scattering (DLS, 90Plus Particle Sizer, Brookhaven Instruments, Holtsville, NY, USA) as described previously (11,15).

PNC Concentration Determination

PNC yield was determined by a colorimetric assay based on the detection of lactic acid monomer (22). PEG–PLA samples were hydrolyzed to their monomer state with 5 M NaOH at 80°C overnight and neutralized with 5 M HCl. One ml of 20 wt.% $CuSO_4$ was added to a 1 ml aliquot of the hydrolyzed sample, alongside standards of known concentrations of lactic acid to construct a calibration curve. Samples were diluted to 10 ml, before addition of 1 g of dry $Ca(OH)_2$. After incubation at room temperature for 30 min, samples were centrifuged at 1,000 g for 5 min and 1 ml aliquots of the supernatant were taken. 50 μl of 4 wt.% $CuSO_4$ and 6 ml of sulfuric acid were sequentially added before incubation at 100°C for 5 min. Samples were subsequently cooled to room temperature and 100 μl of *p*-hydroxydiphenyl in 0.5 wt.% NaOH was added before a 30 min incubation at 30°C. Next, the samples were heated to 100°C for 90 s to dissolve excess hydroxydiphenyl. Once the samples cooled to 25°C, the lactic acid concentration was determined with a spectrophotometer at 560 nm.

PNC Morphology Study

PNC morphology was characterized by fluorescence microscopy, transmission electron microscopy (TEM), and scanning electron microscopy (SEM). For fluorescence microscopy, aliquots of PNC were stained with the lipophilic carbocyanine dye, PKH26, *via* established methods (15,23) and then imaged with a Nikon fluorescence microscope equipped with a ×60 oil immersion objective. For TEM, samples were prepared as previously described (15). Briefly, samples were immobilized on TEM mesh grids (Formvar Film 200 Mesh, Electron Microscopy Sciences, Hatfield, PA) and stained with filtered (0.1 μm filter) 2 wt.% uranyl acetate. Grids were imaged on a TEM (JEOL JEM-100CX, West Chester, PA, USA). For SEM sample preparation, PNC aliquots were lyophilized overnight and spread on a sample plate. Samples were sputter coated with platinum and imaged on a field-emission gun (FEG) environmental scanning electron microscope (ESEM, model XL30)

In vivo Circulation and Biodistribution Studies

PNC were loaded with ^{125}I-catalase or ^{125}I-PEG-catalase and were i.v. injected (tail vein, 50 mg polymer/kg bodyweight) into C57/BL6 mice following an IACUC approved protocol that adhered to the "Principles of Laboratory Animal Care" (NIH publication #85-23, revised in 1985). Non-PNC-encapsulated ^{125}I-catalase and ^{125}I-PEG-catalase were also injected. Blood was drawn in 100 μl aliquots at specified increments from 1 min to 3 h by retro-orbital bleeding. At the end of the experiment, mice were sacrificed and harvested organs were washed, weighed and radioactivity measured. Five mice per experimental group were tested. Statistical significance was tested in all studies *via* a *t* test, where *p* values <0.05 were considered significant.

RESULTS

Polymer Characterization

By controlling reaction feed ratios, ring-opening polymerization (ROP) of lactide with a monomethoxy-capped mPEG initiator yielded mPEG-PLA with PLA block MW's of approximately 18,000 and 27,000 Da (see Table I) as determined by ^{1}H-NMR. The resultant wt.% PLA, or "% PLA", defined as the ratio of PLA MW to the total diblock MW, is also shown in Table I. The GPC-determined polydispersity indices of the polymers were both 1.5. MW of the PEG block was kept constant at 5,000 Da. Polymer MW schemes were selected from previous work to formulate either spherical or filamentous PNC loaded with active catalase (15), also outlined in Table I.

The formulation scheme for nanocarrier synthesis and protein encapsulation utilized throughout these studies, and how PEGylation of the cargo may influence this, is illustrated in Fig. 1A–F. A critical parameter of this protective cage delivery system is the diffusivity of the encapsulated enzyme's

Table I. Synthesized Polymer Characterization

Target PLA $\overline{M_n}$	PLA $\overline{M_n}$ [a]	%PLA	PLA $\overline{M_n}$ [b]	PLA $\overline{M_w}$ [a]	PDI	PNC morphology
20,000.0	17,895.6	78.2	23,236.7	36,908.2	1.5	Spherical (sph)
30,000.0	27,091.3	84.4	21,859.0	35,792.4	1.5	Filamentous (fil)

Number and weight average molecular weights ($\overline{M_n}$ and $\overline{M_w}$, respectively) and polydispersities (PDI, defined as $\overline{M_w}/\overline{M_n}$). Actual % PLA, or wt.% PLA, is defined as the ratio of the actual PLA block $\overline{M_n}$ to the entire diblock copolymer $\overline{M_n}$. All diblocks contain a methoxy end-capped 5,000 MW mPEG, which served as the initiator for the ring opening polymerization (ROP) of lactide into PLA. The PNC morphology that results from the indicated polymer compositions is also noted.
[a] Determined by ^{1}H-NMR
[b] Determined by GPC

substrate through the polymer meshwork. This concept is illustrated in Fig. 1G,H. Flux is derived from the solution to Fick's first law of diffusion for planar geometry, summarized in the following equation:

$$\ln\left(1-\frac{2C_r}{C_d}\right) = -\frac{2Ak}{Vl}Dt$$

where C_d and C_r are donor and cumulative receptor cell concentrations, A is cross sectional area of the film at the port between the two cells, k is the partition coefficient, V is the receptor cell volume, l is the film thickness, D is the permeability coefficient, and t is time (19). While the absolute values of each data point fluctuate from each independent experiment (Fig. 1H), the important parameter, the slope of the corresponding trend line, D, is consistently on the same order of magnitude across all experiments. Measurement in this model showed that the normalized permeability coefficient of the catalase substrate, hydrogen peroxide, through the polymer material utilized for these formulations is on the order of 10^{-9} cm^2/s.

PEG-catalase Circulates *In Vivo* Longer than Catalase, But both PEG-catalase and Catalase are Susceptible to Proteolysis

In the first series of experiments we compared free PEG-catalase with naive catalase without loading into PNC. In accord with the literature, tracing of ^{125}I labeled enzyme showed that PEG-catalase remains in the bloodstream at significantly higher levels than naïve catalase after intravenous injection in mice ($P<0.02$ at 1 min post injection and $P<0.001$ thereafter, Fig. 2A). However, *in vitro* analysis showed that both free (non-loaded) PEG-catalase and catalase are rapidly degraded in proteolytic environments (Fig. 2B). Thus, 1 h incubation with 0.2 wt.% pronase caused 99.0±0.8% and 97.3±0.6% loss of activity of PEG-catalase and catalase, respectively. The rate of inactivation was similarly high for both enzymes at this protease concentration, which we typically use for testing the protective effect of PNC. Further, when the protease concentrations were reduced by an order of magnitude, inactivation was still rapid with a 69.5±1.5% (catalase) and 77.8±6.6% (PEG-catalase) loss of activity within 3 h.

Utilization of PEG-catalase Enhances PNC Loading in a Freeze–Thaw Modified Formulation

We monitored loading of ^{125}I-labeled catalase or PEG-catalase into the nano-scale (<500 nm diameter) fraction of formulated PNC particles utilizing the methodology and analyses described in one of our recent studies (15). Fig. 3A shows that the percent of loading by enzyme mass (defined as the percent of catalase added in the primary emulsion that is entrapped within PNC, or loading efficiency) was significantly enhanced for PEG-catalase vs catalase in both spherical

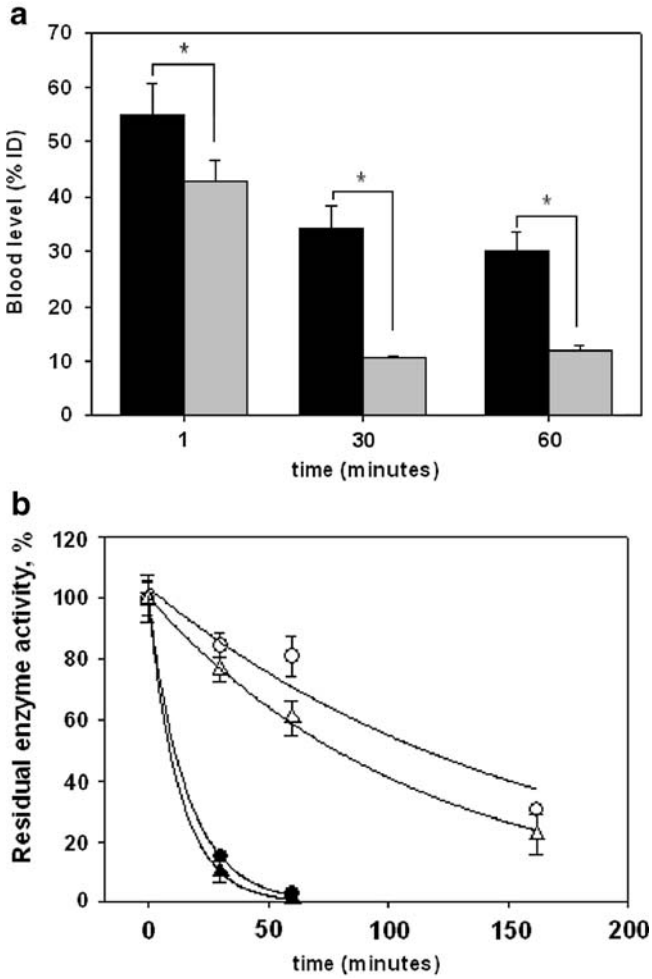

Fig. 2. Circulation and proteolytic resistance of PEG-catalase and unmodified catalase. Circulation studies of PEG-catalase (*black bars*) and unmodified catalase (*gray bars*; **A**). *%ID* indicates percent injected dose. Concentration dependence of enzyme resistance to inactivation by a model protease (**B**). *Circles* correspond to catalase and *triangles* to PEG-catalase. *Black* indicates higher concentration of protease (0.2 wt.%) and *white* indicates a lower concentration (0.02 wt.%). Data are shown as mean value±standard deviation. *Asterisks* indicate statistically significant differences ($P<0.05$).

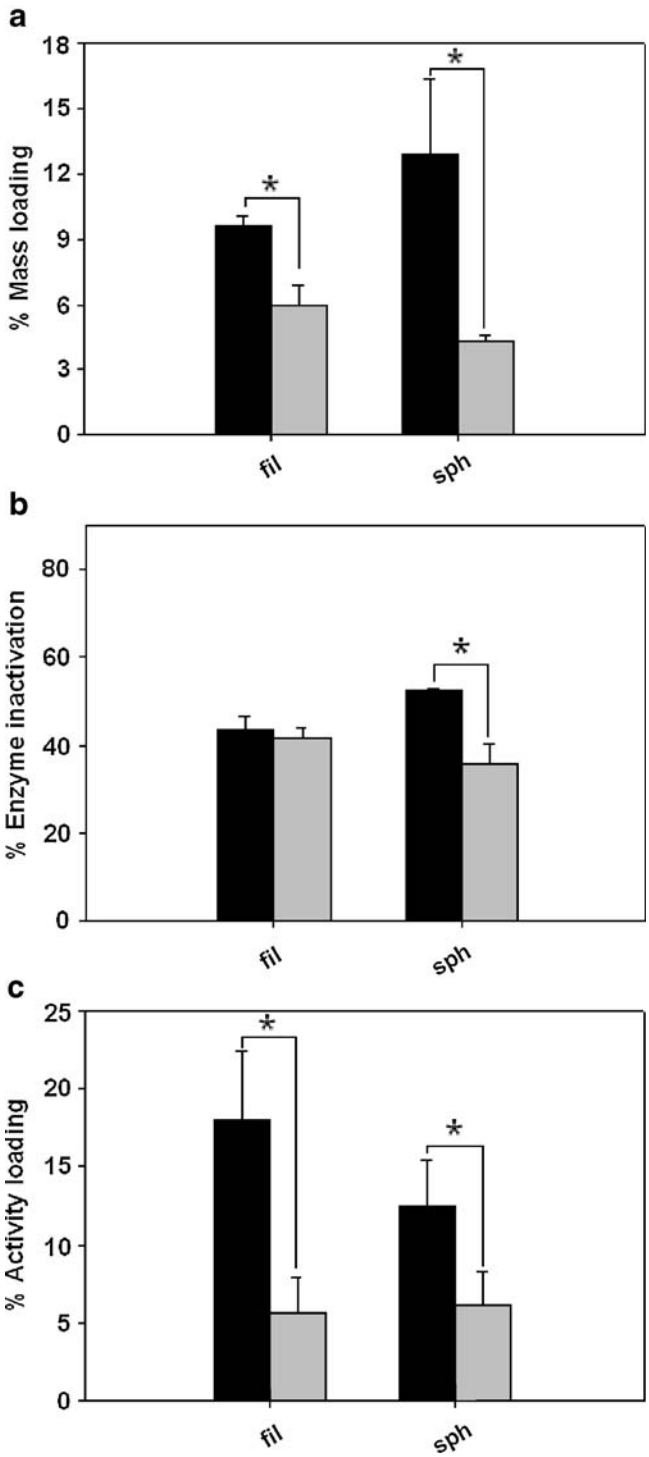

Fig. 3. Enzyme mass and activity loading. Loading by mass is defined as protein mass in PNC divided by the total amount added to the particle prep during the modified emulsion formulation (**A**). The enzymatic activity of catalase lost during the formulation, based on kinetics of H_2O_2 degradation (**B**). Percent of activity of total protein mass added is shown. Loading of catalase into mPEG-PLA PNC based on enzymatic activity (**C**). *Black* indicates PEG-catalase loading, while *gray* is unmodified catalase loading. *Fil* refers to filamentous PNC and *sph* refers to spherical PNC. *Asterisks* indicate statistically significant differences ($P<0.05$).

($P<0.02$) and filamentous PNC ($P<0.001$), by 200% and 100%, respectively.

Retention of enzymatic activity through particle formulation was similar for the PNC encapsulated protein, regardless of PEGylation. It should be noted that there appeared to be little impact of the PEG modification of catalase. Catalase exhibited an activity of 23.3±2.8 kU/mg of protein while PEG-catalase demonstrated 21.5±1.1 kU/mg of protein. The degree of apparent enzyme inactivation during the encapsulation within filamentous PNC was similar for catalase and PEG-catalase. Inactivation was slightly higher for PEG-catalase relative to catalase loaded into spherical PNC (Fig. 3B). It is conceivable that redistribution of the PEG-catalase cargo from the PNC surface into the polymer matrix/PNC interior may in theory augment diffusional limitations of substrate conversion, thereby overestimating PEG-catalase inactivation (see "Discussion").

In order to quantify loaded activity, we defined percent loading as:

$$\%\ \text{Loading} = \left(\frac{\text{activity recovered in PNC}}{\text{total activity, post formulation}}\right) \times (\%\ \text{apparent catalase inactivation})$$

where % apparent catalase inactivation factors in activity lost during the formulation process (15). This method of loaded-catalase quantification provides an ultimate measure of enzyme loading, i.e. total enzymatic activity associated with the PNC, taking into account formulation-induced inactivation. Thus, for both spherical and filamentous PNC, activity loading of PEG-catalase was significantly higher than that of naïve catalase ($P<0.03$, Fig. 3C).

Loading of PEG-catalase Does Not Alter PNC Morphology

In previous studies, we characterized the profound effect of PEGylated diblock copolymer amphiphilicity (and thus the ratio of PEG to PLA) on PNC morphology (15). Thus it was plausible that loading a PEG-enzyme might impact polymer control of PNC structure. Nevertheless, dynamic light scattering (DLS, Fig. 4C) and scanning electron microscopy (SEM, Fig. 4A,B) revealed no marked impact of PEG-enzyme on the size of spherical particles: i.e., the mean diameter of PNC loaded with PEG-catalase or catalase was ~350 nm. Similarly, transmission electron microscopy (TEM) and fluorescence microscopy revealed virtually identical morphologies for filamentous PNC loaded with either PEG-catalase or catalase (Fig. 4E,F). Cross sectional diameters varied between 60 and 70 nm for filamentous carriers with either cargo.

Final PNC concentration in the nano-scale fraction of the particles was determined by quantitative analysis of lactic acid content after complete hydrolysis of the PLA–PEG polyester carriers. Absolute mass yield is calculated based on the fact that PEG and PLA exist in equimolar amounts in the polymer backbone:

$$\text{Diblock polymer mass yield} = \left\{\frac{x\ (\text{g, PLA})}{\text{MW}_{\text{PLA}}\ (\text{g/mol, PLA})} \times [\text{MW}_{\text{PEG}}\ (\text{g/mol, PEG})]\right\} + [x\ (\text{g, PLA})]$$

According to this analysis, there was a small, yet significant ($P<0.001$) increase in mass yield of PNC loaded with PEG-catalase

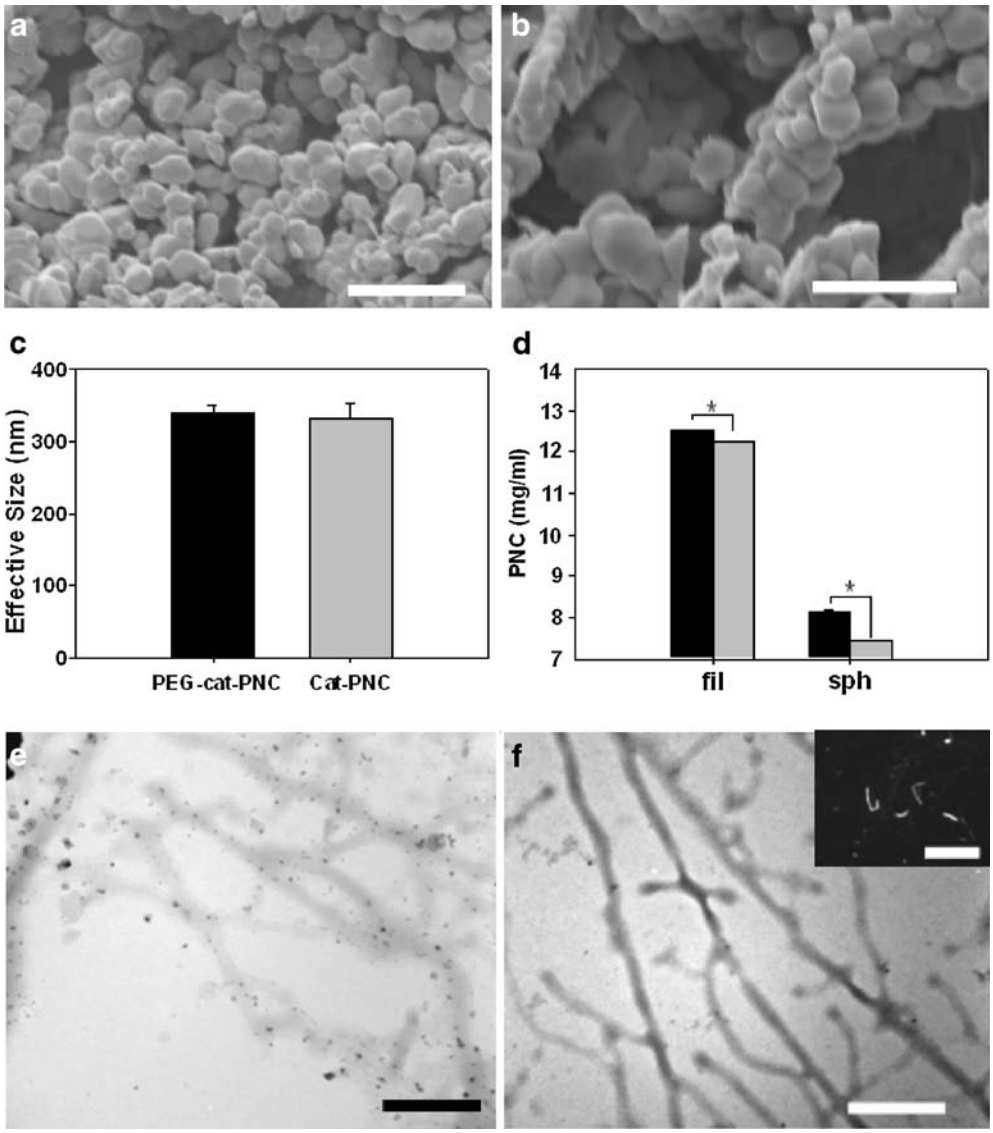

Fig. 4. Morphology of PNC with different enzyme cargoes. SEM images of spherical PNC loaded with either catalase (**A**) or PEG-catalase (**B**). *Scale bar* is 2 μm. Sizing of spherical PNC was determined by DLS (**C**). Note that *cat* = catalase. Mass yield of PNC was determined by PLA content and all particle preps were re-suspended in 1 ml PBS (**D**). TEM images of filamentous PNC with either catalase (**E**) or PEG-catalase (**F**) encapsulated. *Scale bar* is 500 nm. *Inset* shows confocal fluorescence microscopy image of filamentous PNC obtained with a ×60 oil-immersion objective. Staining was with the lipophilic carbocyanine dye, PKH26 intercalated into the PNC polymer. *Scale bar* of *inset* is 5 μm. *Asterisks* indicate statistically significant differences ($P<0.05$).

compared to catalase for both filamentous and spherical carriers (Fig. 4D). Similar to previous results (15), the ultimate yield of filamentous carriers was higher than that of spherical PNC.

PEG-catalase Loaded in PNC is More Resistant to Proteases than Catalase Loaded in PNC

We used an *in vitro* test of protease inactivation to compare the kinetics of proteolytic inactivation of PEG-catalase and catalase when loaded in PNC (Fig. 5A). Protection was determined after a 1 h incubation of the PNC in a protease solution, as this time interval was previously determined to be adequate to distinguish PNC-encapsulated enzyme protection from that of non-encapsulated enzymes (15). PNC-loaded PEG-catalase demonstrated markedly higher resistance to proteolysis than PNC-loaded catalase. This effect was most pronounced with spherical PNC, providing more than a two-fold higher protection of PEG-catalase relative to catalase ($P<0.005$). Filamentous PNC also provided a significantly higher protection of PEG-catalase compared to catalase ($P<0.01$).

PEG-catalase-PNC and Catalase-PNC Circulate in Mice

In order to test the potential utility of these formulations for intravascular drug delivery, ^{125}I-labeled catalase or PEG-catalase loaded within PNC were injected intravenously in mice (Fig. 5B). Both formulations demonstrated significantly elevated levels in the blood relative to free catalase within the

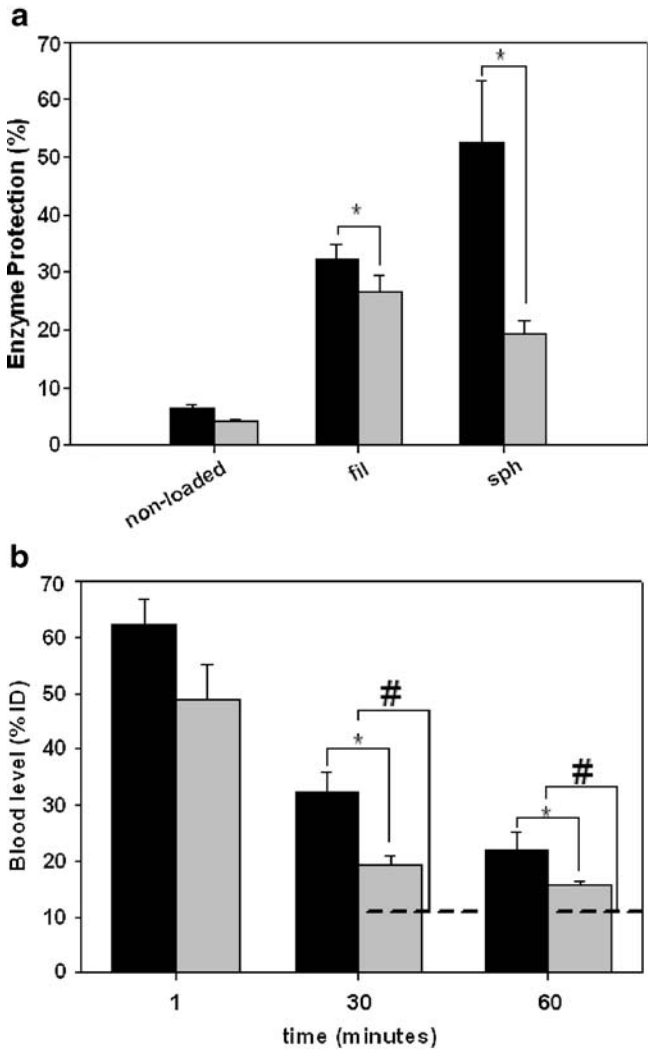

Fig. 5. Protective effect of PNC against external proteases and pharmacokinetics in mice. Protective effect against external protease degradation of PNC-loaded enzymes (**A**). Black indicates PEG-catalase loaded PNC, while gray bars indicate catalase loaded PNC. *Non-loaded* (*far left*) refers to enzyme incubated with empty PNC. Circulation of PEG-catalase-PNC (*black bars*) and unmodified catalase-PNC (*gray bars*) where % ID represents the percent of injected dose remaining in the bloodstream (**B**). *Asterisks* indicate a statistically significant difference between PEG-catalase-PNC and catalase-PNC, while *number signs* indicate a statistically significant difference between both PNC preparations and unloaded catalase (*dashed line*).

first hour post injection ($P<0.001$). Therefore, the circulation time of PNC loaded with either enzyme demonstrate a significant improvement relative to naive catalase that is not loaded within PNC (Fig. 5B, dashed line).

DISCUSSION

Protein drugs represent a rapidly growing area of research, yet their utility is often limited by inefficient delivery and high cost. Efficient and effective encapsulation of active therapeutic enzymes, such as catalase, into polymer nanocarriers that improve cargo delivery and protection from inhibitors and proteases may help overcome this problem. To date, the most successful attempts at encapsulation of catalytically *active* catalase into PNC have utilized a freeze–thaw modified double emulsion technique (11). In this study we tested the hypothesis that PEG-catalase loads more efficiently than catalase into PEG–PLA PNC when such a formulation is used (Fig. 1). This would seem to be the case as our PNC preparations of different morphologies loaded at a far higher efficiency when PEG-catalase was utilized. The same trends in both loading and protection were also observed with PNC formulated from several other different molecular weight PEG–PLA copolymers that we tested (data not shown).

The relatively mild chemical modification of enzymes appears to be a rather plausible solution to enhancing loading of potent biotherapeutics such as catalase into PNC, particularly if production of this delivery system were to reach an industrial scale. PEG modification has long been utilized in pharmaceutics to enhance aqueous solubility, stability and circulation time, as well as reduce recognition by defense systems in the body (24–29). PEG itself has been utilized as a stabilizer for loading small proteins (e.g., chymotrypsin, MW ~25 kDa) into polymer microspheres (30). Other studies examined the feasibility of covalently modifying small (on the order of 50 kDa or less) enzymes or proteins with PEG and loading of these into PLGA *micro*spheres (31–34). PEGylation of catalase is thought to occur primarily *via* lysine residues, with approximately 40 molecules of PEG per molecule of enzyme (as stated by the supplier, Sigma) in the preparations used in this study. At this extent of modification, PEGylation has minimal impact on specific activity of catalase, wherein both unmodified and PEGylated catalase exhibited specific activities on the order of 20 kU/mg protein. Protocols for such chemical modifications of enzymes have long been documented in the literature (25–27,35) and many PEGylated enzymes, catalase included, are commercially available, thus suggesting that this would be a relatively simple modification to implement in an industrial setting.

Our data show that use of PEG-catalase provides higher PNC loading and resistance to protease degradation than unmodified catalase. This trend was similar for both spherical and filamentous PNC, yet an interesting result of PNC morphology can be noted. For instance, while inactivation of PEG-catalase loaded into filamentous PNC was minimal and indistinguishable from that of catalase, the gain in protease resistance was less impressive than in the case of spherical PNC. This outcome suggests that there exists a limit to filamentous PNC protection of its loaded protein, possibly due to the small (~60 nm diameter) cross section. This feature translates into a smaller protective barrier, or in other words, less polymer material between the encapsulated enzyme and any external proteases. Similarly, in the case of spherical PNC, the apparent inactivation of PEG-catalase from formulation was slightly higher than that of catalase. This apparent inactivation may be a reflection of an increase in the diffusion path length of the diffusing enzyme substrate H_2O_2 that results from deeper encapsulation of PEG-catalase within the PNC. For enzymes deeply embedded within the PNC, the polymer thickness that must be traversed in the sphere is approximately equal to R (the radius of the sphere). However, for the filamentous PNC, this value is equal to r (the radius of the filament cross section). From analysis of the DLS and electron microscopy data, R is approximately 150 nm while r is only 30 nm. This is exacerbated when one

considers possible material limitations. For instance, polymer membrane diffusion studies suggest that there may be a minor diffusion limitation for H_2O_2 through the biomaterial matrix since the permeability coefficient through PEG–PLA is on the order of 10^{-9} cm^2/s (Fig. 1H), compared to 10^{-8} cm^2/s (14) through a cell lipid bilayer. While this difference is small, if the utilization of PEG-catalase results in deeper embedment within the PNC, it is plausible that there may be a modest increase in diffusion barrier, i.e. access of the substrate to the encapsulated enzyme. Given the rapid kinetics of catalase activity, even a minor diffusion barrier could result in some degree of *apparent* inactivation. Overall, this does not seem to be a major limiting factor and is consistent with the superior resistance of PEG-catalase to protease degradation when loaded within spherical PNC.

Mechanism and consequences of the enzyme cargo inactivation are worth further studies. Inactivation may result from protein degradation or unfolding. The latter scenario seems plausible, since protein conformational changes are known to happen at solvent/water interfaces, such as those that occur with the double emulsion utilized (36). This is in addition to the "apparent" inactivation due to diffusion limitations of the enzyme substrate that result from the encapsulating nanocarrier material itself, discussed above.

It is widely believed that PEGylation of enzymes offers many solutions to the limitations of protein therapeutics, including prolongation of circulation, facilitation of intracellular delivery and protection against inactivation (24,25,27,35,37–41). Our results on prolonged circulation of PEG-catalase relative to catalase (Fig. 2A) are consistent with the literature. However, our data show that PEG-catalase and catalase showed very similar susceptibilities to proteolysis, independent of protease concentration (Fig. 2B). Of note, PEGylation of fibrinogen did not prevent its proteolysis (42–44). It is conceivable that the proteolytic sensitivity of a PEG-protein depends on the nature and concentration of a protein and a protease. Perhaps at a high extent of modification multiple PEG chains can hinder protein susceptibility to proteases. Similarly, very high MW PEG chains could be grafted onto protein surfaces. These approaches were applied to dextran, where all samples were still ultimately degraded, but enzymatic degradation kinetics slowed with increasing MW and/or extent of PEG modification (45). This PEG coating enhancement would be similar to natural sugars that are observed in the case of heavily glycosylated lysosomal enzymes. However, coupling multiple PEG chains, itself, can inactivate the modified biotherapeutics. In some instances, higher degrees of PEG modification can sacrifice enzyme stability (46). Ultimately, PEG may serve as a kinetic barrier to proteases, yet this effect can be saturated in protease-rich environments like lysosomes. This is most evident when non-loaded PEG-catalase is compared alongside enzymes loaded within PNC that demonstrate a six to tenfold enhancement in protease resistance. Several groups studied the utility of branched PEG modified proteins (37,39,47–49), yet their effectiveness in terms of protease resistance in more concentrated environments has yet to be determined. The loading of such branched-PEG enzymes into PNC has great potential and would be an interesting extension to this finding.

Spherical PNC in the sub-500 nm range are readily internalized when targeted to appropriate cell surface receptors (8) and thus are plausible candidates for intracellular delivery. Furthermore, PNC of this size circulate well enough to target specific cell types when decorated with an affinity moiety, i.e. a peptide, antibody, antibody fragment, aptamer, etc. This is evident when one notes that these PNC, without any targeting ligands, circulate on the order of hours, while similar PNC decorated with targeting antibodies traffic to their specified destination within minutes of injection (13). Thus it would seem that the PEG-catalase-PNC, of approximately the same size as unmodified catalase-PNC, are prime candidates for systemic targeted therapeutics. Circulation studies show that there is a definite enhancement in circulation over non-loaded catalase when either PEG-catalase or catalase is encapsulated within PNC.

Further *in vivo* studies on asymmetrical PNC, particularly filamentous carriers are of potentially great impact, given the recent discoveries with similar systems (50,51). For *nano* filamentous carriers, there is tremendous drug loading capacity afforded by their long, micron scale length. Yet, the fact that they retain their *nano* status in terms of their cross sectional diameter, can result in very long circulating carriers with the potential for prolonged therapy (50). Furthermore, their high surface area to volume ratio indicates a high potential for surface decoration with targeting epitopes relative to the carrier mass and thus has tremendous potential for drug targeting.

CONCLUSION

This study demonstrates a new application for PEGylated enzymes, namely loading within polymer *nano*carriers of unique filamentous and spherical morphologies. The goal of this study was to maximize encapsulation and minimize catalase surface absorption, and thus protease accessibility to the loaded enzyme, in PNC formulations. Enzymes modified with PEG succeed in this area, as well as in enhancing protein mass loading. Thus, a simple and well characterized modification results in a therapeutic enzyme-nanocarrier delivery system well suited for intravascular delivery.

ACKNOWLEDGEMENT

This work was supported by grants from the National Institutes of Health (NIH #'s HL007954, HL073940-01-A1, HL087036 and PO1-HL079063). We thank Tony Lowman and the Centralized Materials Characterization Facility and Industry Consortium of Drexel University for assistance with NMR and SEM studies and Dennis Discher of the University of Pennsylvania for GPC studies.

REFERENCES

1. S. M. Moghimi, A. C. Hunter, and J. C. Murray. Long-circulating and target-specific nanoparticles: theory to practice. *Pharmacol. Rev.* **53**:283–318 (2001).
2. S. M. Moghimi, and J. Szebeni. Stealth liposomes and long circulating nanoparticles: critical issues in pharmacokinetics, opsonization and protein-binding properties. *Prog. Lipid Res.* **42**:463–478 (2003) doi:10.1016/S0163-7827(03)00033-X.
3. E. Roux, M. Lafleur, E. Lataste, P. Moreau, and J. C. Leroux. On the characterization of pH-sensitive liposome/polymer complexes. *Biomacromolecules*. **4**:240–248 (2003) doi:10.1021/bm025651x.

4. V. R. Muzykantov. Targeting of superoxide dismutase and catalase to vascular endothelium. *J. Control. Release*. **71**:1–21 (2001) doi:10.1016/S0168-3659(01)00215-2.
5. M. Christofidou-Solomidou, A. Scherpereel, R. Wiewrodt, K. Ng, T. Sweitzer, E. Arguiri, V. Shuvaev, C. C. Solomides, S. M. Albelda, and V. R. Muzykantov. PECAM-directed delivery of catalase to endothelium protects against pulmonary vascular oxidative stress. *Am. J. Physiol. Lung Cell. Mol. Physiol.* **285**: L283–L292 (2003).
6. B. D. Kozower, M. Christofidou-Solomidou, T. D. Sweitzer, S. Muro, D. G. Buerk, C. C. Solomides, S. M. Albelda, G. A. Patterson, and V. R. Muzykantov. Immunotargeting of catalase to the pulmonary endothelium alleviates oxidative stress and reduces acute lung transplantation injury. *Nat. Biotechnol.* **21**:392–398 (2003) doi:10.1038/nbt806.
7. K. Nowak, S. Weih, R. Metzger, R. F. Albrecht 2nd, S. Post, P. Hohenberger, M. M. Gebhard, and S. M. Danilov. Immunotargeting of catalase to lung endothelium *via* anti-angiotensin-converting enzyme antibodies attenuates ischemia-reperfusion injury of the lung *in vivo*. *Am. J. Physiol. Lung Cell. Mol. Physiol.* **293**:L162–L169 (2007) doi:10.1152/ajplung.00001.2007.
8. S. Muro, X. Cui, C. Gajewski, J. C. Murciano, V. R. Muzykantov, and M. Koval. Slow intracellular trafficking of catalase nanoparticles targeted to ICAM-1 protects endothelial cells from oxidative stress. *Am. J. Physiol. Cell. Physiol.* **285**:C1339–C1147 (2003).
9. A. M. Klibanov. Enzyme stabilization by immobilization. *Anal. Biochem.* **93**:1–25 (1979) doi:10.1016/S0003-2697(79)80110-4.
10. V. P. Torchilin, E. G. Tischenko, V. N. Smirnov, and E. I. Chazov. Immobilization of enzymes on slowly soluble carriers. *J. Biomed. Mater Res.* **11**:223–235 (1977) doi:10.1002/jbm.820110208.
11. T. D. Dziubla, A. Karim, and V. R. Muzykantov. Polymer nanocarriers protecting active enzyme cargo against proteolysis. *J. Control. Release*. **102**:427–439 (2005) doi:10.1016/j.jconrel.2004.10.017.
12. R. Langer. Drug delivery and targeting. *Nature*. **392**:5–10 (1998).
13. T. D. Dziubla, V. V. Shuvaev, N. K. Hong, B. J. Hawkins, M. Madesh, H. Takano, E. A. Simone, M. T. Nakada, A. Fisher, S. M. Albelda, and V. R. Muzykantov. Endothelial targeting of semipermeable polymer nanocarriers for enzyme therapies. *Biomaterials*. **29**:215–227 (2008)doi:10.1016/j.biomaterials.2007.09.023.
14. L. C. Seaver, and J. A. Imlay. Hydrogen peroxide fluxes and compartmentalization inside growing Escherichia coli. *J. Bacteriol.* **183**:7182–7189 (2001) doi:10.1128/JB.183.24.7182-7189.2001.
15. E. A. Simone, T. D. Dziubla, F. Colon-Gonzalez, D. E. Discher, and V. R. Muzykantov. Effect of polymer amphiphilicity on loading of a therapeutic enzyme into protective filamentous and spherical polymer nanocarriers. *Biomacromolecules*. **8**:3914–3921 (2007) doi:10.1021/bm700888h.
16. A. Hillgren, and M. Alden. Differential scanning calorimetry investigation of formation of poly(ethylene glycol) hydrate with controlled freeze-thawing of aqueous protein solution. *J. Appl. Polym. Sci.* **91**:1626–1634 (2004) doi:10.1002/app.13249.
17. C. Branca, S. Magazu, G. Maisano, F. Migliardo, P. Migliardo, and G. Romeo. Hydration study of PEG/water mixtures by quasi elastic light scattering, acoustic and rheological measurements. *J. Phys. Chem. B*. **106**:10272–10276 (2002) doi:10.1021/jp014345v.
18. A. M. Bellocq. Phase equilibria of polymer-containing microemulsions. *Langmuir.* **14**:3730–3739 (1998) doi:10.1021/la970821q.
19. C. L. Bell, and N. A. Peppas. Water, solute and protein diffusion in physiologically responsive hydrogels of poly (methacrylic acid-g-ethylene glycol). *Biomaterials*. **17**:1203–1218 (1996) doi:10.1016/0142-9612(96)84941-6.
20. V. V. Shuvaev, T. Dziubla, R. Wiewrodt, and V. R. Muzykantov. Streptavidin-biotin cross linking of therapeutic enzymes with carrier antibodies: nanoconjugates for protection against endothelial oxidative stress. *Methods Mol. Biol.* **283**:3–19 (2004).
21. R. F. Beers Jr., and I. W. Sizer. A spectrophotometric method for measuring the breakdown of hydrogen peroxide by catalase. *J. Biol. Chem.* **195**:133–140 (1952).
22. S. B. Barker, and W. H. Summerson. The colorimetric determination of lactic acid in biological material. *J. Biol. Chem.* **138**:535–554 (1941).
23. P. Dalhaimer, F. S. Bates, and D. E. Discher. Single molecule visualization of stable, stiffness-tunable, flow-conforming worm micelles. *Macromolecules*. **36**:6873–6877 (2003) doi:10.1021/ma034120d.
24. J. S. Beckman, R. L. Minor Jr., C. W. White, J. E. Repine, G. M. Rosen, and B. A. Freeman. Superoxide dismutase and catalase conjugated to polyethylene glycol increases endothelial enzyme activity and oxidant resistance. *J. Biol. Chem.* **263**:6884–6892 (1988).
25. A. Abuchowski, J. R. McCoy, N. C. Palczuk, T. van Es, and F. F. Davis. Effect of covalent attachment of polyethylene glycol on immunogenicity and circulating life of bovine liver catalase. *J. Biol. Chem.* **252**:3582–3586 (1977).
26. P. S. Pyatak, A. Abuchowski, and F. F. Davis. Preparation of a polyethylene glycol: superoxide dismutase adduct, and an examination of its blood circulation life and anti-inflammatory activity. *Res. Commun. Chem. Pathol. Pharmacol.* **29**:113–127 (1980).
27. J. S. Beckman, R. L. Minor Jr., and B. A. Freeman. Augmentation of antioxidant enzymes in vascular endothelium. *J. Free Radic. Biol. Med.* **2**:359–365 (1986) doi:10.1016/S0748-5514(86)80036-8.
28. T. Minko, P. V. Paranjpe, B. Qiu, A. Lalloo, R. Won, S. Stein, and P. J. Sinko. Enhancing the anticancer efficacy of camptothecin using biotinylated poly(ethylene glycol) conjugates in sensitive and multidrug-resistant human ovarian carcinoma cells. *Cancer Chemother. Pharmacol.* **50**:143–150 (2002) doi:10.1007/s00280-002-0463-1.
29. S. V. Vinogradov, T. K. Bronich, and A. V. Kabanov. Self-assembly of polyamine-poly(ethylene glycol) copolymers with phosphorothioate oligonucleotides. *Bioconjug. Chem.* **9**:805–812 (1998) doi:10.1021/bc980048q.
30. I. J. Castellanos, R. Crespo, and K. Griebenow. Poly(ethylene glycol) as stabilizer and emulsifying agent: a novel stabilization approach preventing aggregation and inactivation of proteins upon encapsulation in bioerodible polyester microspheres. *J. Control. Release*. **88**:135–145 (2003) doi:10.1016/S0168-3659(02)00488-1.
31. M. Diwan, and T. G. Park. Pegylation enhances protein stability during encapsulation in PLGA microspheres. *J. Control. Release*. **73**:233–244 (2001) doi:10.1016/S0168-3659(01)00292-9.
32. M. Diwan, and T. G. Park. Stabilization of recombinant interferon-alpha by pegylation for encapsulation in PLGA microspheres. *Int. J. Pharm.* **252**:111–122 (2003) doi:10.1016/S0378-5173(02)00636-1.
33. W. Wasfi Al-Azzam, E. A. Pastranna, B. King, J. Méndez, and K. Griebenow. Effect of the covalent modification of horseradish peroxidase with poly(ethylene glycol) on the activity and stability upon encapsulation in polyester microspheres. *J. Pharm. Sci.* **94**:1808–1819 (2005) doi:10.1002/jps.20407.
34. T. H. Kim, H. Lee, and T. G. Park. Pegylated recombinant human epidermal growth factor (rhEGF) for sustained release from biodegradable PLGA microspheres. *Biomaterials*. **23**:2311–2317 (2002) doi:10.1016/S0142-9612(01)00365-9.
35. A. Abuchowski, T. van Es, N. C. Palczuk, and F. F. Davis. Alteration of immunological properties of bovine serum albumin by covalent attachment of polyethylene glycol. *J. Biol. Chem.* **252**:3578–3581 (1977).
36. D. J. McClements. Protein-stabilized emulsions. *Curr. Opin. Colloid Interface Sci.* **9**:305–313 (2004) doi:10.1016/j.cocis.2004.09.003.
37. I. Fuke, T. Hayashi, Y. Tabata, and Y. Ikada. Synthesis of poly (ethylene glycol) derivatives with different branchings and their use for protein modification. *J. Control. Release*. **30**:27–34 (1994) doi:10.1016/0168-3659(94)90041-8.
38. R. Federico, A. Cona, P. Caliceti, and F. M. Veronese. Histaminase PEGylation: preparation and characterization of a new bioconjugate for therapeutic application. *J. Control. Release*. **115**:168–174 (2006) doi:10.1016/j.jconrel.2006.07.020.
39. F. M. Veronese, C. Monfardini, P. Caliceti, O. Schiavon, M. D. Scrawen, and D. Beer. Improvement of pharmacokinetic, immunological and stability properties of asparaginase by conjugation to linear and branched monomethoxy poly (ethylene glycol). *J. Control. Release*. **40**:199–209 (1996) doi:10.1016/0168-3659(95)00185-9.
40. F. M. Veronese, P. Caliceti, A. Pastorino, O. Schiavon, L. Sartore, L. Banci, and L. M. Scolaro. Preparation, physico-chemical and pharmacokinetic characterization of monomethoxypoly(ethylene glycol)-derivatized superoxide dismutase. *J. Control. Release*. **10**:145–154 (1989) doi:10.1016/0168-3659(89)90025-4.
41. F. Fuertges, and A. Abuchowski. The clinical efficacy of poly (ethylene glycol)-modified proteins. *J. Control. Release*. **11**:139–148 (1990) doi:10.1016/0168-3659(90)90127-F.

42. D. Dikovsky, H. Bianco-Peled, and D. Seliktar. Defining the role of matrix compliance and proteolysis in three-dimensional cell spreading and remodeling. *Biophys. J.* **94**:2914–2525 (2008).
43. M. Gonen-Wadmany, L. Oss-Ronen, and D. Seliktar. Protein-polymer conjugates for forming photopolymerizable biomimetic hydrogels for tissue engineering. *Biomaterials*. **28**:3876–3886 (2007) doi:10.1016/j.biomaterials.2007.05.005.
44. D. Dikovsky, H. Bianco-Peled, and D. Seliktar. The effect of structural alterations of PEG-fibrinogen hydrogel scaffolds on 3-D cellular morphology and cellular migration. *Biomaterials*. **27**:1496–1506 (2006) doi:10.1016/j.biomaterials.2005.09.038.
45. H.-C. Chiu, C. Konak, P. Kopeckova, and J. Kopecek. Enzymatic degradation of poly(ethylene glycol) modified dextrans. *J. Bioact. Compat. Polym.* **9**:388–410 (1994) doi:10.1177/088391159400900403.
46. X. Y. Xiong, K. C. Tam, and L. H. Gan. Effect of enzymatic degradation on the release kinetics of model drug from Pluronic F127/poly(lactic acid) nano-particles. *J. Control. Release*. **108**:263–270 (2005) doi:10.1016/j.jconrel.2005.08.005.
47. O. Schiavon, P. Caliceti, P. Ferruti, and F. M. Veronese. Therapeutic proteins: a comparison of chemical and biological properties of uricase conjugated to linear or branched poly (ethylene glycol) and poly(*N*-acryloylmorpholine). *Farmaco*. **55**:264–269 (2000) doi:10.1016/S0014-827X(00)00031-8.
48. C. Monfardini, O. Schiavon, P. Caliceti, M. Morpurgo, J. M. Harris, and F. M. Veronese. A branched monomethoxypoly (ethylene glycol) for protein modification. *Bioconjug. Chem.* **6**:62–69 (1995) doi:10.1021/bc00031a006.
49. Y. Ren, H. Zhang, and J. Huang. Synthesis and cytotoxic activity of platinum complex immobilized by branched polyethylene glycol. *Bioorg. Med. Chem. Lett.* **15**:4479–4483 (2005) doi:10.1016/j.bmcl.2005.07.019.
50. Y. Geng, P. Dalhaimer, S. Cai, R. Tsai, M. Tewari, T. Minko, and D. E. Discher. Shape effects of filaments *versus* spherical particles in flow and drug delivery. *Nat. Nano.* **2**:249–255 (2007) doi:10.1038/nnano.2007.70.
51. S. Cai, K. Vijayan, D. Cheng, E. M. Lima, and D. E. Discher. Micelles of different morphologies-advantages of worm-like filomicelles of PEO-PCL in paclitaxel delivery. *Pharm. Res.* **24**:2099–2109 (2007).